Eur Biophys J (1992) 21, 345–348

European Biophysics Journal

Conformational change of a synthetic amyloid analogue des[Ala^{21,30}]A42 upon binding to octyl glucoside micelles

Ilona Laczkó-Hollósi [1]*, Miklós Hollósi [2], Virginia M.-Y. Lee [3], and Henry H. Mantsch [4]

[1] Institute of Biophysics, Biological Research Center, Szeged, Hungary
[2] Institute of Organic Chemistry, L. Eötvös University, Budapest, Hungary
[3] University of Pennsylvania, Philadelphia, USA
[4] National Research Council Canada, Institute for Biodiagnostic Winnipeg, Manitoba, Canada

Received September 5, 1992/Accepted in revised form September 16, 1992

Abstract. The secondary structure of a synthetic amyloid fragment des [Ala^{21,30}]A42 was studied by circular dichroism and Fourier transformed infrared spectroscopy. Measurements were performed in trifluoroethanol/water and octyl β-D-glucopyranoside solutions. The spectra of the peptide in trifluoroethanol indicate a high percentage of α-helical structure. However, in octyl glucoside, at and above the critical micelle concentration, the peptide adopts a β-sheet conformation. Secondary structure analysis yields a predominant (>70%) β-sheet content. Our data suggest that the peptide backbone or polar side groups of des[Ala^{21,30}]A42 interact with the sugar-coated surface of micelles, which promotes an α to β conformational transition.

Key words: Alzheimer's disease – Amyloid A4 – Conformational change – Octyl glucoside

Introduction

Alzheimer's disease is characterized by progressive accumulation of fibrous, proteinaceous aggregates in blood vessels and the brain (Tomlinson and Corsellis 1984). The major component of these aggregates is a 4.2 kDa amyloid peptide called β protein or A4. A4 is formed by abnormal proteolytic cleavage of its precursor which is a 695-residue N-glycosylated membrane protein displaying the features of cell surface receptors (Kang et al. 1987). A4, containing 42 or 43 amino acids, is located near the C-terminus of the precursor and its hydrophobic 29-42 segment reaches into the membrane (Dyrks et al. 1988; Weidemann et al. 1989).

A42: H-Asp-Ala-Glu-Phe-Arg-His-Asp-Ser-Gly-Tyr-Glu-Val-His-His-Gln-Lys-Leu-Val-Phe-Phe-*Ala*^{21}-Glu-Asp-Val-Gly-Ser-Asn-Lys-Gly-*Ala*^{30}-Ile-Ile-Gly-Leu-Met-Val-Gly-Gly-Val-Val-Ile-Ala-OH

* *Correspondence to:* I. Laczkó-Hollósi, Ins. Biophysics, Biological Research Center, H-6701 Szeged, P.O. Box. 521, Hungary

The membrane-spanning domain probably forms an α-helix in vivo (Dyrks et al. 1988; Hilbich et al. 1991 a). In amyloid deposition, however, the A4 peptides are present in a β-sheet form (Kirschner et al. 1987). Thus, a transition from a partly α-helical conformation into a β-sheet is the prerequisite for deposit formation in vivo. Recent circular dichroism (CD) studies have shown that fragments of synthetic A4 have a tendency to adopt multiple conformations in solution (Hollósi et al. 1989; Kirschner et al. 1987).

This paper reports CD and Fourier transform infrared (FT-IR) spectroscopic measurements on des[Ala^{21,30}]A4, an analogue of A4, in trifluoroethanol (TFE), TFE-water mixtures and in aqueous octyl β-D-glucopyranoside (OG) solutions. Deletion of alanines in positions 21 and 30 resulted in an enhanced solubility, relative to the poor solubility of A42 and A43(A42Thr) (Hilbich et al. 1991 a, b). OG, a non-ionic detergent, was found to be effective in solubilizing membrane proteins (Andreu 1982; Horwitz and Bok 1987; Werner and Reithmeier 1985). The purpose of this study is to gain more information about the mechanism of the "pleating" process of amyloid peptides.

Materials and methods

des[Ala^{21,30}]A42 was synthesized on solid phase using a BioSearch SAM2 automated synthesizer. The synthesis was accomplished on PAL-resin and Fmoc-N-terminal-protected amino acids were employed. Single couplings with a 6-fold molar excess of preformed symmetrical anhydrides in dichloromethane-N,N dimethylformamide (DMF) (1:1 v/v) were performed for 2 h each (Atherton et al. 1978). The protecting Fmoc-groups were cleaved with 30% piperidine in toluene-DMF (1:1 v/v) solution. For cleavage of the peptide from resin, a trifluoroacetic acid-thioanisole 95:5 v/v mixture was used. After cleavage, the peptide was dialyzed in 1000 MWCO tubing against water for 2 hours. The peptide was almost immediately precipitated in the dialysis tubing as the water

content increased inside. Purification of the peptide was carried out by high performance liquid chromatography as described earlier (Ötvös et al. 1989). A4 was eluted at 32% CH_3CN. Amino acid analysis resulted in the expected amino acid composition. The integrity of the N-terminal decapeptide sequence of des[Ala^{21,30}]A42 was further verified by Edman sequencing. In the FAB mass spectrum measured with a VG Analytical ZAB 2-SE instrument, the appearance of the $(M+H)^+$ signal at m/z 4372 also gave support to the structure of this analogue. CD measurements were carried out on a Jasco J720 dichrograph. Unless otherwise mentioned, freshly prepared solutions were used. The peptide showed good solubility in TFE but was not fully soluble in water or PBS at pH 7.4. To prepare the aqueous OG solutions, the peptide samples were wet with a tiny amount of TFE prior to dissolving them in the appropriate solution of OG. The final TFE concentration never exceeded 1%. Octyl β-D-glucopyranoside (OG) was purchased from Sigma. The peptide concentration of the samples was 0.5 mg/ml, the length of the cuvette was 0.2 mm. Mean residue ellipticity $[\Theta]_{MR}$ was expressed in degrees cm^2/dmol using a mean residue weight of 112.

Infrared spectra were recorded on a Digilab FTS-60 instrument at a resolution of 2 cm^{-1}. All measurements were performed at room temperature from sample aliquots containing 100 µg peptide in 50 µl solvent. At this concentration the peptide is only sparingly soluble in water at neutral pH, however it becomes soluble by addition of organic solvents (TFE, acetonitrile, dimethyl sulfoxide), or by adjusting the pH to 2 or 12. Infrared spectra of the solvents were obtained under identical conditions and were substracted from the spectra of the peptide in the relevant solvent. Owing to HPLC purification, the peptide was present as a trifluoroacetate salt with a sharp infrared band at 1673 cm^{-1}. Therefore, it was additionally purified for IR spectroscopy by passing it over an ion exchange minicolumn (Amberlite IR-45).

Percentages of secondary structures were calculated with the protein secondary structure estimation program SSE-338 purchased from Jasco. This program is based on reference spectra measured by Yang et al. (1986), an average number of helical residues, $\bar{n}_\alpha = 10$ was assumed. Hydropathicity of the peptide sequence was analyzed by the method of Kyte and Doolittle (1982). For prediction of the secondary structure, an improved version of the Chou-Fasman method was used (Argos et al. 1978).

Results

CD measurements were performed in TFE, TFE/water and 0.4–2.5% aqueous OG solutions. In 100% TFE, des[Ala^{21,30}]A42 shows a spectrum typical of proteins with a high degree of helicity (Fig. 1). The curve-analyzing method resulted in 64% α-helix and 36% random conformation. However, at lower TFE concentrations the shape of the spectra reflected an increasing contribution of β-sheet structure. The calculation resulted in 12% α-helix, 71% β-sheet and 17% random conformation in 10% TFE solution.

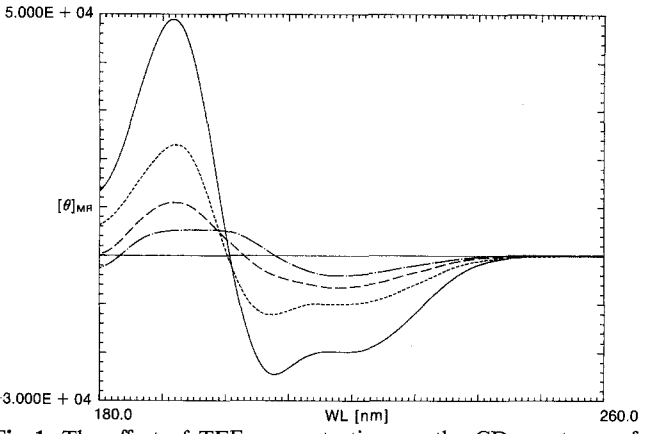

Fig. 1. The effect of TFE concentration on the CD spectrum of des[Ala^{21,30}]A42. (——), 100%; (-----), 50%; (– – –), 25%; (– · – ·), 10% TFE. Peptide concentration: 0.5 mg/ml

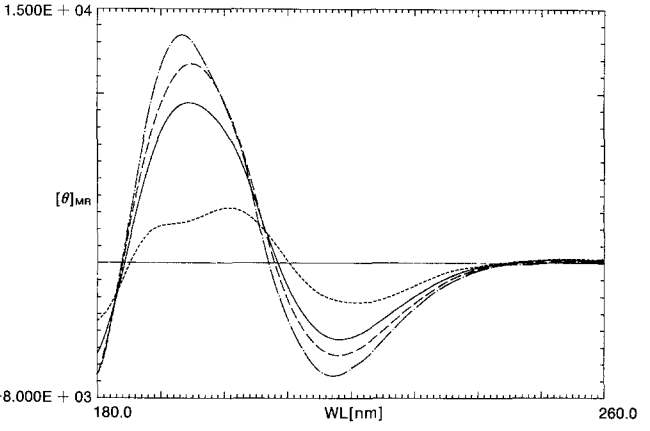

Fig. 2. The effect of N-octyl-D-glucopyranoside concentration on the CD spectrum of des[Ala^{21,30}]A42. (-----), 0.4%; (——), 0.73%; (– – –), 1.25%; (– · – ·), 2.5%. Peptide concentration: 0.5 mg/ml

CD spectra were also measured in aqueous OG solutions. The critical micelle concentration (CMC) of octyl glucoside at room temperature is 25 mM (0.73%). The CD spectrum of OG in water shows a positive band around 183 nm which derives from the optical activity of the glucose moiety (Johnson 1987). Therefore the CD spectra in OG solution were corrected using the spectra of OG solutions measured at the same concentration. Figure 2 shows the CD spectra of des[Ala^{21,30}]A42 in solutions of different (0.4–2.5%) OG concentrations. Below the CMC (at 0.4%) the shape and the low intensity of the CD bands reflect the presence of various conformations. However, at the CMC, a sharp increase in the magnitude of the positive band occurs and the spectrum resembles that of β-sheet structures. The increase of the negative band is less characteristic than that of the positive band. The explanation is that below the CMC (e.g. at 0.4%) the small amount of β-sheet gives a definite negative CD band near 220 nm while the positive band of the β-sheet is suppressed by the negative CD of the unordered conformation. The decomposition of the spectrum measured in 0.73% OG solution shows the dominance of the β conformation (~80%). Further increase of the detergent

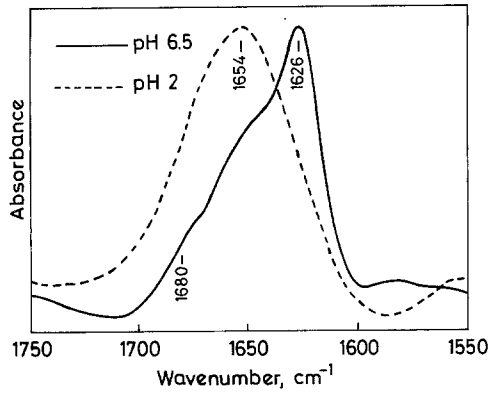

Fig. 3. FT-IR spectra in the amide I region of des[Ala^{21,30}]A42 in water (D_2O) at pH 2 (-----), and at pH 6.5 (——)

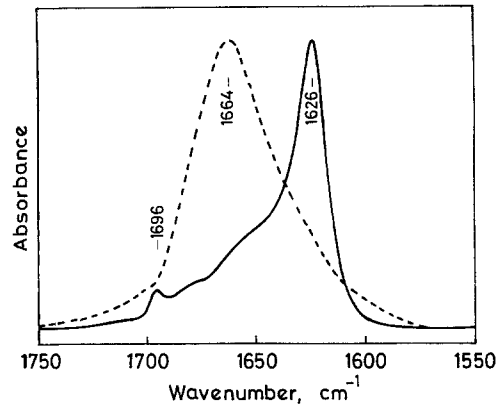

Fig. 4. FT-IR spectra in the amide I region of des[Ala^{21,30}]A42 in water (D_2O, pH 6.5) in the presence of OG micelles (2.5%) (——), and as a solution in DMSO (-----)

concentration results in a small increase of the band intensities with a concomitant blue shift.

Figure 3 shows the infrared spectra in the region of the amide I bands (amide C=O stretching bands) of des[Ala^{21,30}]A42 as a fine suspension in water (D_2O) at neutral pH and as a true solution at pH 2. The broad amide I band centered around 1654 cm^{-1} observed at pH 2 is typical of proteins or peptides lacking any ordered secondary structure (Fraser et al. 1991). On the other hand, the strong IR band at 1626 cm^{-1}, found in the spectrum of the aqueous suspension at neutral pH, is highly characteristic of β-sheet structures (Surewicz and Mantsch 1988). The presence of a weaker band around 1680 cm^{-1}, indicates that the β-sheets are antiparallel (Krimm and Bandekar 1986). In the latter spectrum there is also a broad residual band at 1650 cm^{-1}, revealing the existence of an appreciable amount of amide groups in peptide segments not involved in the formation of the β-sheets. The IR-based observation that the β-sheet structure of des[Ala^{21,30}]A42 is destroyed at pH 2 is in agreement with results of recent CD studies on 1–28, 1–39 and 1–42 fragments of A4 (Barrow et al. 1992). The β-sheet conformation was found to be favoured between pH 4 and 7. Shorter fragments show a more complicated behaviour. FT-IR studies of fragment 15–28 indicated stable β-sheet formation below pH 10, while fragment 19–28 showed a predominantly random conformation at pH 7 and a mixture of random and β-sheet conformation at pH 2 (Fraser et al. 1991).

The IR spectrum of des[Ala^{21,30}]A42 in pure TFE (not shown) has only a major amide I band centered at 1658 cm^{-1}, characteristic of α-helical structures. On addition of water the β-sheet content increases as revealed by the enhanced intensity of the low frequency band originating from β-sheet structures.

The solid trace in Figure 4 shows the spectrum of a micellar solution of des[Ala^{21,30}]A42 in 2.5% OG. It is a textbook example of a spectrum of antiparallel β-sheets with bands of very small intensity between the major band at 1626 cm^{-1} and the high frequency component band at 1696 cm^{-1}. The peptide is readily soluble in dimethyl sulfoxide. This solvent is known to disrupt intra and intermolecular hydrogen bonds in proteins and peptides as all amide N–H groups seek to form H-bonds to the S=O group of the solvent. The broken trace in Figure 4 shows only a single amide I band at 1664 cm^{-1}, characteristic of proteins and peptides in this solvent (Jackson and Mantsch 1991).

Discussion

An analysis of des[Ala^{21,30}]A42 sequence by hydropathic profiling and secondary structure prediction methods has led to a model containing two helical domains: one largely hydrophilic helix (residues 1–20), and a second hydrophobic helix (residues 30–42). The N-terminal helical domain is interrupted by a short segment (residues 6–9) with high β-turn-forming potential (Hilbich et al. 1991 b; Kirschner et al. 1987). The two helical domains also have a β-sheet-forming tendency. As a consequence, the two regions may adopt both α-helical and β-sheet conformation, depending on environmental effects. In spite of the great difference in the concentration of the solutions used for CD and FT-IR studies (see Materials and methods), both methods support the model based on the prediction. In TFE, which is well known to have an α-helix promoting effect and may mimic the lipid environment of the interior of the cell membrane (Urry et al. 1971), the main part of the molecule adopts α-helical conformation. In OG, at and above the CMC, the peptide is present mainly in a β-sheet conformation. According to data from the literature, the CD spectra of membrane proteins measured in OG above the CMC represent the native secondary structure (Horwitz and Bok 1987; Werner et al. 1985), which, in most cases, is an amphipathic α-helix one for the membrane-spanning parts of proteins (Eisenberg et al. 1984). The α-helix stabilizing effect of OG was attributed to the interaction of the non-polar tails of the detergent molecules with the hydrophobic side chains of proteins (Brunden et al. 1984; Visser and Blout 1971). Minor conformational effects of OG in other cases were revealed by CD measurements but the appearance of a predominant β-sheet structure in OG solution has not been reported yet. Our results support a β-sheet inducing and stabilizing effect of OG on des[Ala^{21,30}]A42. At and above the CMC, the OG molecules form micelles with a

polar surface made up from the glucose head groups, which can mimic the glycoprotein- or glycolipid-covered regions of the membrane surface. We hypothesize that the amide groups of the backbone or the polar side-chain functions interact with this surface through ionic and mainly H-bonding interactions, resulting in a β-forming core which promotes an α to β conformational transition and intersheet stacking. According to the infrared spectrum of a more concentrated solution of the peptide in 2.5% aqueous OG, the β-sheet is antiparallel and persists essentially through the whole molecule, which suggests a β-sheet-β-turn-β-sheet conformation interacting through its hydrophylic N-terminal part with the micelles.

Amyloid formation may arise as a consequence of membrane damage and from polypeptides that are not integrated into membranes (Weidemann et al. 1989). Recent studies have demonstrated that the transmembrane domain of A4 has a high tendency to aggregate in the absence of membranes (Dyrks et al. 1988). The spectroscopic studies reported here give a possible explanation of this process: a transition of α-helix to β-sheet initiated and preserved by the sugar coated surface of the cell membrane or membrane fragments.

Acknowledgements. The authors wish to thank Dr. L. Ötvös, Wistar Institute, Philadelphia for his assistance in the synthesis of des[Ala^{21,30}]A42.

References

Andreu JM (1982) Interaction of tubulin with non-denaturing amphiphiles. EMBO J 1:1105–1110

Atherton E, Fox H, Harkiss D, Logan CJ, Sheppard RC, Williams BJ (1978) A mild procedure for solid phase peptide synthesis: use of fluorenylmethoxycarbonyl-amino acids. J Chem Soc Chem Comm pp 537–539

Argos P, Hanei M, Garavito RM (1978) The Chou-Fasman secondary structure prediction method with an extended data base. FEBS Lett 93:19–24

Barrow CJ, Yasuda A, Kenny PTM, Zagorski MG (1992) Solution conformations and aggregational properties of synthetic amyloid β-peptides of Alzheimer's disease. J Mol Biol 225:1075–1093

Brunden KR, Uratani Y, Cramer WA (1984) Dependence of the conformation of a calicin E1 channel-forming peptide on acidic pH and solvent polarity. J Biol Chem 259:7682–7687

Dyrks T, Weidemann A, Multhaup G, Salbaum JM, Lemaire HG, Kang J, Müller-Hill B, Masters CL, Beyreuther K (1988) Identification, transmembrane orientation and biogenesis of the amyloid A4 precursor of Alzheimer's disease. EMBO J 7:949–957

Eisenberg D, Schwarz E, Komáromy M, Wall R (1984) Analysis of membrane and surface protein sequences with the hydrophobic moment plot. J Mol Biol 179:125–142

Fraser PE, Nguyen JT, Surewicz WK, Kirschner D (1991) pH-dependent structural transitions of Alzheimer amyloid peptides. Biophys J 60:1190–1201

Hilbich C, Kisters-Woike B, Reed J, Masters CL, Beyreuther K (1991a) Aggregation and secondary structure of synthetic amyloid βA4 peptides of Alzheimer's disease. J Mol Biol 218:149–163

Hilbich C, Kisters-Woike B, Reed J, Masters CL, Beyreuther K (1991b) Human and rodent sequence analogs of Alzheimer's amyloid βA4 share similar properties and can be solubilized in buffers of pH 7.4. Eur J Biochem 201:61–69

Hollósi M, Ötvös L, Jr., Kajtár J, Perczel A, Lee VM-Y (1989) Is amyloid deposition in Alzheimer's disease preceded by an environment-induced double conformational transition? Peptide Res 2:109–113

Horwitz J, Bok D (1987) Conformational properties of the main intrinsic polypeptide (MIP26) isolated from lens plasma membranes. Biochemistry 26:8092–8098

Jackson M, Mantsch HH (1991) Beware of proteins in DMSO. Biochim Biophys Acta 1078:231–235

Johnson WC, Jr. (1987) The circular dichroism of carbohydrates. Adv Carbohydr Chem Biochem 45:73–124

Kang J, Lemaire HG, Unterbeck Ak, Salbaum JM, Masters CL, Grzeschik K-H, Multhaup G, Beyreuther K, Müller-Hill B (1987) The precursor of Alzheimer's disease amyloid A4 protein resembles a cell-surface receptor. Nature 325:733–736

Kirschner DA, Inouye H, Duffy LK, Sinclair A, Lind M, Selkoe DJ (1987) Synthetic peptide homologous to β protein from Alzheimer's disease forms amyloid-like fibrils in vitro. Proc Natl Acad Sci USA 84:6953–6957

Krimm S, Bandekar J (1986) Vibrational spectroscopy and conformation of peptides, plypeptides and proteins. Adv Protein Chem 38:181–364

Kyte J, Doolittle RF (1982) A simple method for displaying the hydrophobic character of a protein. J Mol Biol 157:105–132

Ötvös L, Jr., Elekes I, Lee VM-Y (1989) Solid phase synthesis of phosphopeptides. Int J Pept Protein Res 34:129–133

Surewicz WK, Mantsch HH (1988) New insight into protein secondary structure from resolution-enhanced infrared spectra. Biochim Biophys Acta 952:115–130

Tomlinson BE, Corsellis JAN (1984) Aging and the dementias. In: Adams JH, Corsellis JAN, Duchen JW (eds) Greenfield's Neuropathology, Arnold, London, pp 951–983

Yang JT, Wu C-SC, Martinez HM (1986) Calculation of protein conformation from circular dichroism. Meth Enzymol 130:208–269

Urry DV, Masotti L, Krivacis JR (1971) Circular dichroism of biological membranes. I. Mitochondria and red blood cell ghost. Biochim Biophys Acta 241:600–612

Visser L, Blout ER (1971) Elastase. II. Optical properties and the effects of sodium dodecyl sulfate. Biochemistry 10:743–752

Weidemann A, König G, Bunke D, Fischer P, Salbaum JM, Masters CL, Beyreuther K (1989) Identification, biogenesis and localization of precursors of Alzheimer's disease A4 amyloid protein. Cell 57:115–126

Werner PK, Reithmeier RA (1985) Molecular characterization of the human erythrocyte anion transport protein in octyl glucoside. Biochemistry 24:6375–6381